

Review

Not peer-reviewed version

---

# Potentials-Based Computer Modelling of Lanthanide Doped Mixed Metal Fluorides and Oxides for Optical Applications

---

[Robert Adam Jackson](#)\*

Posted Date: 15 January 2025

doi: 10.20944/preprints202501.1189.v1

Keywords: potentials; computer modelling; defects, dopants; fluorides; oxides; lanthanide doping



Preprints.org is a free multidisciplinary platform providing preprint service that is dedicated to making early versions of research outputs permanently available and citable. Preprints posted at Preprints.org appear in Web of Science, Crossref, Google Scholar, Scilit, Europe PMC.

Copyright: This open access article is published under a Creative Commons CC BY 4.0 license, which permit the free download, distribution, and reuse, provided that the author and preprint are cited in any reuse.

Review

# Potentials-Based Computer Modelling of Lanthanide Doped Mixed Metal Fluorides and Oxides for Optical Applications

Robert A Jackson

School of Chemical and Physical Sciences, Keele University, Keele, Staffordshire ST5 5AX;  
r.a.jackson@keele.ac.uk

**Abstract:** This article presents a review of the field of potentials-based computer modelling as applied to the doping by lanthanides, of a range of metal oxides and fluorides, with a view to enhancing various properties for optical applications. The following host compounds are considered: BaLiF<sub>3</sub>, BaY<sub>2</sub>F<sub>8</sub>, SrAl<sub>2</sub>O<sub>4</sub> and LiNbO<sub>3</sub>.

**Keywords:** potentials; computer modelling; defects; dopants; fluorides; oxides; lanthanide doping

## 1. Introduction

Mixed metal fluorides and oxides, doped with lanthanide ions, have a range of applications in optical devices. Computer modelling, based on the use of interatomic potentials, has been widely used to predict the location of dopant ions and the preferred form of charge compensation (if needed), which can then be used to help in synthesis and characterisation of the doped materials. This article looks at work done by the author and collaborators over several years, and it is hoped that it will be useful reference point for future work in the field.

The article starts with a section on methodology, discussing interatomic potentials and their derivation, lattice energy minimisation for the prediction of structures and the calculation of crystal properties, and the calculation of defect formation energies, and solution energies for dopants in materials.

The materials chosen are all of importance in device applications. The first two materials, BaLiF<sub>3</sub> and BaY<sub>2</sub>F<sub>8</sub>, are both used in laser applications, and in the case of BaLiF<sub>3</sub>, a range of possible doping sites and charge compensation schemes are possible, and the calculations show that the preferred site depends on the specific dopant. The third material, SrAl<sub>2</sub>O<sub>4</sub>, acts as a phosphor when doped with Dy<sup>3+</sup> and Eu<sup>2+</sup> ions, but the experimental papers do not usually discuss the detailed solid state chemistry involved in the doping, making this system a good candidate for modelling studies. The final material, LiNbO<sub>3</sub>, has many technological applications including when doped with lanthanide ions, but there is disagreement about the location of dopant ions and charge compensation schemes, again making it an excellent material for modelling studies.

## 2. Methodology

All calculations were performed using the GULP code [1] which has been widely used in modelling studies of a range of materials. The code can be used to fit interatomic potentials and to carry out energy minimisation and defect calculations, as described in the sub sections that follow this.

### 2.1. Interatomic Potentials

The computer modelling work presented in this review paper was all performed using interatomic potentials. The Buckingham potential has been employed, augmented with a term to represent the electrostatic interactions between ions, and it has the following form:

$$V(r) = A \exp(-r/\rho) - Cr^{-6} + q_1 q_2 / r$$

where  $A$ ,  $\rho$  and  $C$  are parameters to be obtained by empirical fitting, and  $q_1$ ,  $q_2$  are charges on the interacting ions with ' $r$ ' being the interionic distance. The shell model has been employed, usually for anions, to represent ionic polarizability, with the ionic charge being split between a core and shell, connected by a harmonic spring [2].

For each compound described the procedure for derivation of potentials is discussed in that section, but in general, empirical fitting has been used, where potentials are fitted to crystal structures, and (where available) crystal properties including elastic and dielectric constants.

The justification for using potentials-based calculations when quantum mechanical methods are increasingly available is that very detailed calculations can be performed on complex materials in a shorter time than would be possible with, for example, DFT calculations. This is further discussed in the conclusions, where a paper comparing the methods is cited.

### 2.2. Lattice Energy Minimisation

Lattice energy minimisation can be used to calculate structures corresponding to a minimum in the lattice energy.

The total lattice energy is written as a sum of interactions between ions (described by interatomic potentials):

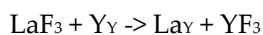
$$E_{\text{latt}} = \sum V(r)$$

Then, by adjusting the structure (either the lattice parameters or atomic positions or both), the minimum energy structure is obtained. Note that a well derived potential would be expected to reproduce the structure without significant structural adjustment.

### 2.3. Defect Formation Energies and Solution Energies

The main interest in this paper is in calculating the formation energy of dopants in a given structure, but in addition, intrinsic defect energies (mainly formation energies of vacancies and interstitials) are also important. These have all been calculated by the Mott-Littleton method [3] in which a spherical region (region I) is defined surrounding the defect, in which interactions are summed explicitly, and an outer region (region IIB) which is treated as a dielectric continuum. An interface region (IIA) ensures continuity between the inner and outer regions. There is a detailed discussion of the method, including a useful diagram, in our paper on  $\text{UO}_2$  [4].

However, defect formation energies do not, on their own, describe the overall solution process, and to do that, solution energies are defined. For example, consider doping  $\text{BaY}_2\text{F}_8$  with  $\text{La}^{3+}$  ions, assuming doping at the  $\text{Y}^{3+}$  site (although this is considered in more detail in section 3.2). A possible solution process can be written as:



The energy of formation of  $\text{La}^{3+}$  at the  $\text{Y}^{3+}$  site is calculated, and then combined with the lattice energies of  $\text{LaF}_3$  and  $\text{YF}_3$  to give the solution energy for the process:

$$E_{\text{sol}} = E(\text{La}_Y) + E_{\text{latt}}(\text{YF}_3) - E_{\text{latt}}(\text{LaF}_3)$$

In the following results sections, the calculation of solution energies is discussed in more detail.

## 3. Results

Four materials have been chosen from those previously studied. The two mixed metal fluorides,  $\text{BaLiF}_3$  and  $\text{BaY}_2\text{F}_8$  are both used as host materials for lanthanide dopants, and they differ in the preferred doping sites, information that is useful in synthesis of the doped materials. The two mixed metal oxides have different applications.  $\text{SrAl}_2\text{O}_4$  is used for phosphor applications when doped with

lanthanides, but as is noted, the experimental papers are not usually concerned with dopant sites and charge compensation. LiNbO<sub>3</sub> has many applications, but in the case of lanthanide doping there is disagreement on doping sites and charge compensation, and calculations are used to address this issue.

3.1. BaLiF<sub>3</sub>

BaLiF<sub>3</sub> is a material which adopts the inverted perovskite structure. It has interesting properties as a potential laser material when doped with both divalent and trivalent cations.

Derivation of a potential for the material was carried out using empirical fitting, and unusually, a range of experimental properties were available to use in the fit, including elastic and dielectric constants. Table 1, see [5], shows calculated properties compared with experimental values, and Table 2 gives the potential parameters. It is seen from Table 1 that very good agreement is obtained between the calculated and experimental values.

Table 1. Perfect lattice properties for BaLiF<sub>3</sub>.

Property	Calculated	Experimental (references in [4])
Lattice energy (eV)	-34.83	-
Lattice parameter a (Å)	3.995	3.995
Elastic constants (dyn cm <sup>-2</sup> )		
c <sub>11</sub>	12.99	12.98
c <sub>12</sub>	4.76	4.65
c <sub>44</sub>	4.76	4.87
Dielectric constants		
ε <sub>0</sub>	11.70	11.71
ε <sub>∞</sub>	2.25	2.25

Table 2. Potential parameters obtained by empirical fitting.

Short-range interactions	A (eV)	ρ(Å)	C (eV Å <sup>6</sup> )
Ba <sub>core</sub> –F <sub>shell</sub>	3090.2	0.2987	0.0
Li <sub>core</sub> –F <sub>shell</sub>	400.6	0.2736	0.0
F <sub>shell</sub> –F <sub>shell</sub>	1153.0	0.1365	0.0

Shell model parameters

$Y = q(F_{shell}) = -2:321 |e|$

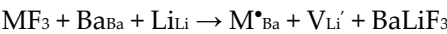
$k(F_{core} - F_{shell}) = 48:40 \text{ eV Å}^{-2}$

Turning now to doping with the trivalent ions La<sup>3+</sup>, Y<sup>3+</sup> and Nd<sup>3+</sup>, it is noted that these ions can potentially substitute at either the Ba<sup>2+</sup> site or the Li<sup>+</sup> site, but that charge compensation will be

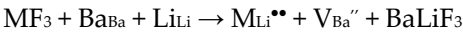
required. This situation is considered in detail in [6], where the following forms of charge compensation are proposed:

- (i) formation of a  $\text{Li}^+$  vacancy.
- (ii) formation of a  $\text{F}^-$  interstitial,
- (iii) formation of a  $\text{Ba}^{2+}$  vacancy,
- (iv)  $\text{Li}^+$  substitution at a  $\text{Ba}^{2+}$  site.

Four possible solution schemes are proposed for solution at each of the  $\text{Ba}^{2+}$  and  $\text{Li}^+$  sites, and it was found that for  $\text{La}^{3+}$  and  $\text{Nd}^{3+}$ , the most favourable solution scheme involves substitution at the  $\text{Ba}^{2+}$  site with compensation by  $\text{Li}^+$  vacancies (where Kroger-Vink notation has been used [7]):



For  $\text{Y}^{3+}$ , the most favourable substitution site is  $\text{Li}^+$ , with compensation by  $\text{Ba}^{2+}$  vacancies:



The difference in the predicted behaviour of  $\text{La}^{3+}$  and  $\text{Nd}^{3+}$  compared with  $\text{Y}^{3+}$  is rationalised in terms of the mean distances between the dopants and the nearest  $\text{F}^-$  ion in the corresponding  $\text{MF}_3$  structures. These predictions are of use when synthesising doped  $\text{BaLiF}_3$ , an example of which is co-doping with  $\text{Yb}^{3+}$  and  $\text{Er}^{3+}$  for X-ray dosimetry and imaging applications [8], in that a knowledge of the preferential location of dopant ions and any charge compensation can be used to guide the synthesis of the doped materials.

3.2.  $\text{BaY}_2\text{F}_8$

$\text{BaY}_2\text{F}_8$  is a promising material for applications in optical devices, and experimental papers have reported doping with Er, Pr, Tm and Dy [9]. While it might be expected that these ions would dope at the  $\text{Y}^{3+}$  site, solution energy calculations were carried out to confirm this [10].

As with  $\text{BaLiF}_3$ , potentials were obtained by empirical fitting, but in this case only structural information was available. Tables 3 and 4 give, respectively, the structural agreement and the potential parameters themselves. Agreement is within 2%, which is regarded as acceptable when there is limited data to fit to.

Table 3. Structural agreement for  $\text{BaY}_2\text{F}_8$ .

Parameter	Exp. (reference in [9])	Calc.	Diff. (%)
$a/\text{\AA}$	6.9829	6.9519	-0.44
$b/\text{\AA}$	10.5190	10.6686	1.42
$c/\text{\AA}$	4.2644	4.1957	-1.61
$\beta/^\circ$	99.6760	98.3700	-1.31

**Table 4.** Potential parameters obtained by empirical fitting.

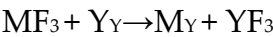
Short-range interactions	A (eV)	$\rho(\text{\AA})$	C (eV $\text{\AA}^6$ )
$Y_{\text{core}} - F_{\text{shell}}$	1653.61	0.3023	0.0
$Ba_{\text{core}} - F_{\text{shell}}$	2311.01	0.3068	0.0
$F_{\text{shell}} - F_{\text{shell}}$	911.69	0.2707	13.80

**Shell model parameters**

$Y = q(F_{\text{shell}}) = -1.378|e|$

$k(F_{\text{core}} - F_{\text{shell}}) = 24.36 \text{ eV } \text{\AA}^{-2}$

Considering doping with lanthanide ions, three solution schemes were considered:  
(i) substitution at the Y3+ site (no charge compensation needed)



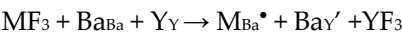
$$E_{\text{sol}} = -E_{\text{latt}}(MF_3) + E(M_Y) + E_{\text{latt}}(YF_3)$$

(ii) substitution at the Ba2+ site (charge compensation by Ba2+ vacancies)



$$E_{\text{sol}} = -2E_{\text{latt}}(MF_3) + 2E(M_{Ba}^{\bullet}) + E(V_{Ba}^{''}) + 3E_{\text{latt}}(BaF_2)$$

(iii) substitution at the Ba2+ site (charge compensation by Ba2+/Y3+ substitution)



$$E_{\text{sol}} = -E_{\text{latt}}(MF_3) + E(M_{Ba}^{\bullet}) + E(Ba_Y') + E_{\text{latt}}(YF_3)$$

Solution energies for each of these schemes are reported in Table 5, for Pr, Nd, Tb, Dy, Er, and Tm. In the case of Nd and Tb doped BaY2F8, they were also the subject of a separate combined experimental and modelling study [11]. It is clear from the table that doping at the Y3+ site is energetically preferred in all cases.

**Table 5.** Solution energies in eV for selected dopants in BaY2F8.

Solution scheme:	$M_Y$	$(M_{Ba}^{\bullet}) - (V_{Ba}^{''})$	$(M_{Ba}^{\bullet}) - (Ba_Y')$
Pr	0.72	4.38	2.60
Nd	0.64	4.78	2.71
Tb	0.32	6.46	3.08
Dy	0.36	6.75	3.29
Er	0.25	6.32	3.32

Tm                                      0.34                                      6.76                                      3.50

In conclusion, for lanthanide doping in BaY<sub>2</sub>F<sub>8</sub>, solution energy calculations confirm that doping occurs at the Y site, which is important in guiding synthesis of the doped materials.

3.3. SrAl<sub>2</sub>O<sub>4</sub>

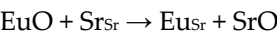
SrAl<sub>2</sub>O<sub>4</sub> when doped with Eu<sup>2+</sup> and Dy<sup>3+</sup> ions, acts as a phosphor material, and is widely used in applications like emergency signs. In experimental papers (see e.g. [12]), it is widely assumed that doping occurs at the Sr<sup>2+</sup> site, but there is often no discussion of how the charge is compensated if Dy<sup>3+</sup> ions also substitute at these sites. This makes doped SrAl<sub>2</sub>O<sub>4</sub> an excellent candidate for a computer modelling study [13].

As with the other materials, potentials were needed, but in this case, they were available from the literature [14]. Table 6 compares experimental and calculated lattice parameters for SrAl<sub>2</sub>O<sub>4</sub>. It is noted that the agreement is not perfect, but these potentials were chosen so that the other relevant oxide phases needed to calculate solution energies could also be calculated.

Table 6. Structural agreement for SrAl<sub>2</sub>O<sub>4</sub>.

Parameter	Exp. (reference in [12])	Calc.	Diff. (%)
<i>a</i> /Å	8.44365	8.49801	0.64
<i>b</i> /Å	8.82245	8.03433	2.40
<i>c</i> /Å	5.15964	5.25031	1.76
$\alpha=\gamma/^\circ$	90.0	90.0	0.0
$\beta/^\circ$	93.411	92.425	-0.99

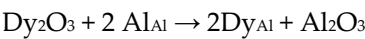
Now doping by Eu<sup>2+</sup> and Dy<sup>3+</sup> ions is considered. In the case of just doping an Eu<sup>2+</sup> ion at a Sr<sup>2+</sup> site, the solution scheme is assumed to be:



And the solution energy is calculated from:

$$E_{\text{sol}} = [E(\text{Eu}_{\text{Sr}}) + E_{\text{latt}}(\text{SrO})] - [E_{\text{latt}}(\text{EuO})]$$

The solution energy is calculated to be 0.06 eV per dopant ion, which suggests doping by Eu<sup>2+</sup> ions alone is favourable. However, it is now necessary to consider Dy<sup>3+</sup> ion doping. In terms of ion charges, it might be reasonably assumed that the Dy<sup>3+</sup> ion might substitute at the Al<sup>3+</sup> site, with the following solution scheme:



The solution energy for this process is calculated to be 1.72 eV per Dy<sup>3+</sup> ion, suggesting that doping at this site would be energetically feasible. However, this is not the assumption made in the experimental papers, where doping at the Sr<sup>2+</sup> site is assumed. If doping by Sr<sup>2+</sup> ions alone is considered, a possible scheme, with charge compensation by Sr<sup>2+</sup> vacancies is:



The solution energy for this process is calculated to be 3.08 eV per Dy<sup>3+</sup> ion, considerably higher than for solution at the Al<sup>3+</sup> site, suggesting that doping at this site would be unlikely. The question

then is whether co-doping of  $\text{Eu}^{2+}$  and  $\text{Dy}^{3+}$  ions at the  $\text{Sr}^{2+}$  site leads to a lower solution energy. The following solution scheme is considered:



The solution energy for this process is calculated to be 2.08 eV per dopant ion, which shows that co-doping does reduce the solution energy, and that this solution scheme, involving  $\text{Sr}^{2+}$  vacancies, can be used to explain  $\text{Eu}^{2+}$  and  $\text{Dy}^{3+}$  co-doping in  $\text{SrAl}_2\text{O}_4$ .

The calculations presented on  $\text{SrAl}_2\text{O}_4$  are useful in that they enable the question of where dopants substitute, and how charge compensation is most optimally achieved, to be answered, which is a point often ignored in the experimental papers.

### 3.4. $\text{LiNbO}_3$

Lithium niobate,  $\text{LiNbO}_3$  is of interest because of its many technological applications [15]. Doping with a range of cations, including lanthanides, is important for device applications, and computer modelling can help determine where dopants are accommodated, and with which form of charge compensation.

A potential was derived by fitting simultaneously to the structures of  $\text{LiNbO}_3$ ,  $\text{Li}_2\text{O}$  and  $\text{Nb}_2\text{O}_5$  [16] since the oxide phases are important in determining solution energies for various doping schemes. The structure of the ferroelectric phase as determined using this potential is compared with experimental data in Table 7, and it seen that good agreement is obtained. Also discussed in [16] is the calculation of elastic, dielectric and piezoelectric constants, which were not included in the fit, but which compare well with experimental values.

**Table 7.** Structural agreement for  $\text{LiNbO}_3$  (ferroelectric phase).

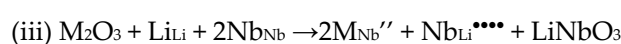
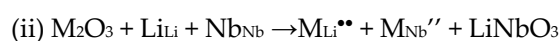
Parameter	Exp. (reference in [15])	Calc.	Diff. (%)
$a=b/\text{\AA}$	5.1474	5.1559	0.16
$c/\text{\AA}$	13.8561	13.6834	-1.2

Before considering doping, it is important to consider intrinsic defects, because lithium niobate is lithium deficient (or has niobium in excess), and any model should support this observation. This is considered in detail in [17], and the following conclusions were reached:

- (i) The non-stoichiometry is explained by antisite or interstitial niobium compensated by lithium or niobium vacancies.
- (ii) Of the various possible schemes, the lowest energy is obtained for antisite niobium compensated by lithium vacancies, as in the following reaction:



Now considering lanthanide dopants, lanthanides can potentially dope at either the  $\text{Li}^+$  or  $\text{Nb}^{5+}$  site, with more than one charge compensation scheme in each case. The following solution schemes were considered:





In Table 8, calculated solution energies for the lanthanide series for each scheme are given.

**Table 8.** Solution energies for lanthanide doping in LiNbO<sub>3</sub>.

Scheme (i)	Scheme (ii)	Scheme (iii)	Scheme (iv)
Ce 5.32	0.85	3.06	6.26
Pr 5.34	0.83	2.85	8.66
Nd 5.40	0.84	2.85	6.04
Sm 5.63	1.09	3.30	6.43
Eu 5.55	1.44	3.03	8.40
Gd 5.48	1.41	2.16	8.85
Tb 5.51	0.98	2.41	6.90
Dy 5.22	0.85	2.69	5.70
Ho 5.33	0.84	2.81	8.19
Er 5.23	1.53	2.82	8.00
Tm 5.18	1.22	2.66	8.09
Yb 5.21	0.90	2.69	5.77
Lu 5.17	0.75	2.67	5.93

It is clear that in all cases scheme (ii), which involves doping at both sites (also known as self-compensation) is favoured. This is an intriguing result when compared with experimental data obtained using EXAFS [18], which although applied to Zn dopants, finds very low occupancy of the Nb site. This result is discussed in the context of analysis of the EXAFS data [19]. A similar study, but using a lanthanide dopant, would be of great interest here.

The calculations presented here on lanthanide doped LiNbO<sub>3</sub> show that there are a range of schemes for doping, including dopant sites and charge compensation mechanisms, and that there is still scope for research in this area, given the experimental findings referred to.

**4. Discussion and Conclusions**

The four materials chosen in this review show the range of research done on lanthanide doping in mixed metal fluorides and oxides. In each case, solution energies are calculated which enable predictions to be made about the energetically optimal location of dopants, and favoured charge compensation schemes. This information can be useful in synthesis of the doped materials, and in characterising them (for example, [11]). The method used, based on interatomic potentials, enables complex systems to be modelled, but increasingly, *ab initio* methods (often based on Density Functional Theory), are being applied to these materials, and the additional information that they can provide will be of great interest, particularly where electronic properties are concerned. However, a comparison of potentials-based modelling and DFT approaches when applied to Th<sup>4+</sup> incorporation in MgF<sub>2</sub> [20] points to the difficulty in comparing the results of the two methods.

**Acknowledgments:** The author is grateful to the many collaborators who have been involved in the work presented in this review article. They are too many to list individually, but I am particularly grateful to Mário E G Valerio, who introduced me to mixed metal fluoride systems, and whose experimental and theoretical understanding of solid-state materials has been an asset throughout our collaboration.

**Conflicts of Interest:** The author declares no conflicts of interest.

## References

1. Gale, J.D. GULP: A computer program for the symmetry-adapted simulation of solids, *J. Chem. Soc. Faraday. Trans.*, **1997**, 93, 629-637
2. Dick, B.G., Overhauser, A.W. Theory of the dielectric constants of alkali halide crystals, *Physical Review*, **1958**, 112 (1), 90-103
3. Mott, N.F., Littleton, M.J. Conduction in polar crystals. I. Electrolytic conduction in solid salts, *Trans. Faraday Soc.*, **1938**, 34, 485
4. Read, M.S.D., Jackson, R.A. Derivation of enhanced potentials for uranium dioxide and the calculation of lattice and intrinsic defect properties, *J. Nuclear Materials*, **2010**, 406, 293-303
5. Jackson, R.A., Valerio, M.E.G., de Lima, J.F. Computer Modelling of BaLiF<sub>3</sub>: I. Interionic potentials and intrinsic defects, *J. Phys: Condensed Matter*, **1996**, 8, 10931-10937
6. Valerio, M.E.G., de Lima, J.F., Jackson, R.A. Computer Modelling of BaLiF<sub>3</sub>: III. Substitution of La<sup>3+</sup>, Nd<sup>3+</sup> and Y<sup>3+</sup> ions, *Radiation Effects and Defects in Solids*, **1999**, 151(1-4), 1061-1066
7. Kröger, F.A., Vink, H.J. Relations between the Concentrations of Imperfections in Crystalline Solids, *Solid State Physics*, **1956**, 3, 307-435
8. Choudhury, N., Riesen, N., Riesen, H. Yb<sup>3+</sup> and Er<sup>3+</sup> codoped BaLiF<sub>3</sub> nanocrystals for X-ray dosimetry and imaging by upconversion luminescence, *ACS Appl. Nano Mater.*, **2021**, 4, 6659-6667
9. Parisi, D., Toncelli, A., Tonelli, M., Cavalli, E., Bovero, E., Belletti, A. Optical spectroscopy of BaY<sub>2</sub>F<sub>8</sub>:Dy<sup>3+</sup>, *J. Phys: Condensed Matter*, **2005**, 17, 2783.
10. Amaral, J.B., Couto dos Santos, M.A., Valerio, M.E.G., Jackson, R.A. Computer modelling of BaY<sub>2</sub>F<sub>8</sub>: defect structure, rare earth doping and optical behaviour, *Applied Physics B*, 81 (6), **2005**, 81 (6), 841-846
11. Valerio, M.E.G., Ribeiro, V.G., de Mello, A.C.S., dos Santos, M.A.C., Baldochi, S.L., Mazzocchi, V.L., Parente, C.B.R., Jackson, R.A., Amaral, J.B. Structural and optical properties of Nd- and Tb-doped BaY<sub>2</sub>F<sub>8</sub>, *Optical Materials*, **2007**, 30, 184-187
12. Botterman, J., Joos, J.J., Smet, P.F. Trapping and detrapping in SrAl<sub>2</sub>O<sub>4</sub>: Eu, Dy persistent phosphors: Influence of excitation wavelength and temperature, *Physical Review B*, **2014**, 90, 085147
13. Jackson, R.A., Kavanagh, L.A., Snelgrove, R.A. Computer modelling of double doped SrAl<sub>2</sub>O<sub>4</sub> for phosphor applications, *IOP Conf. Ser.: Mater. Sci. Eng.*, **2017**, 169, 012004
14. <http://www.ucl.ac.uk/klmc/Potentials/Library/catlow.lib>
15. Jackson, R.A., Szaller, Z. Recent Progress in Lithium Niobate, *Crystals*, **2020**, 10(9), 780-782
16. Jackson, R.A., Valerio, M.E.G. A new interatomic potential for the ferroelectric and paraelectric phases of LiNbO<sub>3</sub>, *J. Phys: Condensed Matter*, **2005**, 17, 837-843
17. Araujo, R.M., Lengyel, K., Jackson, R.A., Kovács, L., Valerio, M.E.G. A computational study of intrinsic and extrinsic defects in LiNbO<sub>3</sub>, *Journal of Physics: Condensed Matter*, **2007**, 19, 046211
18. Bridges, F., Mackeen, C., Kovács, L. No difference in local structure about a Zn dopant for congruent and stoichiometric LiNbO<sub>3</sub>, *Phys. Rev. B*, **2016**, 94, 014101
19. Valerio, M.E.G., Jackson, R.A., Bridges, F. EXAFS simulations in Zn-doped LiNbO<sub>3</sub> based on defect calculations, *IOP Conf. Ser.: Mater. Sci. Eng.*, **2017**, 169, 012003
20. Jackson, R.A., Valerio, M.E.G. Computer Modelling of Intrinsic Defects and Th Incorporation in MgF<sub>2</sub>: What we can learn from Atomistic Modelling and DFT Approaches, *Journal of Physics: Conference Series*, **2022**, 2298, 012002

**Disclaimer/Publisher's Note:** The statements, opinions and data contained in all publications are solely those of the individual author(s) and contributor(s) and not of MDPI and/or the editor(s). MDPI and/or the editor(s) disclaim responsibility for any injury to people or property resulting from any ideas, methods, instructions or products referred to in the content.